

# Leishmanicidal Effects of Piperlongumine (Piplartine) and Its Putative Metabolites

## Authors

Fernanda de Lima Moreira<sup>1</sup>, Thalita Bachelli Riul<sup>2</sup>, Marcela de Lima Moreira<sup>3</sup>, Alan Cesar Pilon<sup>4</sup>, Marcelo Dias-Baruffi<sup>2</sup>, Márcio S. S. Araújo<sup>3</sup>, Norberto Peporine Lopes<sup>4</sup>, Anderson R. M. de Oliveira<sup>5</sup>

## Affiliations

- 1 Faculdade de Ciências Farmacêuticas de Ribeirão Preto, Universidade de São Paulo, Ribeirão Preto – SP, Brazil
- 2 Departamento de Análises Clínicas, Toxicológicas e Bromatológicas, Faculdade de Ciências Farmacêuticas de Ribeirão Preto, Universidade de São Paulo, Ribeirão Preto – SP, Brazil
- 3 Instituto René Rachou, Fundação Oswaldo Cruz – FIOCRUZ/MG, Belo Horizonte – MG, Brazil
- 4 Núcleo de Pesquisa em Produtos Naturais e Sintéticos (NPPNS), Faculdade de Ciências Farmacêuticas de Ribeirão Preto, Universidade de São Paulo, Ribeirão Preto – SP, Brazil
- 5 Departamento de Química, Faculdade de Filosofia, Ciências e Letras de Ribeirão Preto, Universidade de São Paulo, Ribeirão Preto – SP, Brazil

## Key words

cyclic amides, pipartine, metalloporphyrin, leishmaniasis, selectivity index, piperlongumine, Piperaceae, analogues

received October 14, 2017

revised April 5, 2018

accepted April 15, 2018

## Bibliography

DOI <https://doi.org/10.1055/a-0614-2680>

Published online | Planta Med © Georg Thieme Verlag KG  
Stuttgart · New York | ISSN 0032-0943

## Correspondence

Prof. Dr. Norberto Peporine Lopes  
NPPNS, Faculdade de Ciências Farmacêuticas de Ribeirão Preto, Universidade de São Paulo  
Avenida do Café, s/n, 14040-903 Ribeirão Preto – SP, Brazil  
Phone: + 55 16 36 02 47 07, Fax: + 55 16 36 02 42 43  
[npelopes@fcrp.usp.br](mailto:npelopes@fcrp.usp.br)

 Supporting information available online at  
<http://www.thieme-connect.de/products>

## ABSTRACT

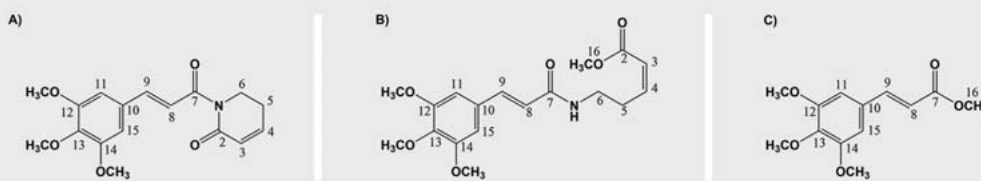
Piperlongumine is an amide alkaloid found in Piperaceae species that shows a broad spectrum of biological properties, including antitumor and antiparasitic activities. Herein, the leishmanicidal effect of piperlongumine and its derivatives produced by a biomimetic model using metalloporphyrins was investigated. The results showed that IC<sub>50</sub> values of piperlongumine in promastigote forms of *Leishmania infantum* and *Leishmania amazonensis* were 7.9 and 3.3 μM, respectively. The IC<sub>50</sub> value of piperlongumine in the intracellular amastigote form of *L. amazonensis* was 0.4 μM, with a selectivity index of 25. The piperlongumine biomimetic derivatives, Ma and Mb, also showed leishmanicidal effects. We also carried out an *in vitro* metabolic degradation study showing that Ma is the most stable piperlongumine derivative in rat liver microsome incubations. The results presented here indicate that piperlongumine is a potential leishmanicidal candidate and support the biomimetic approach for development of new antileishmanial derivatives.

## Introduction

Leishmaniasis is a disease with a broad range of clinical presentations, caused by protozoan parasites from the *Leishmania* genus [1]. The World Health Organization (WHO) estimates approximately 0.7 to 1.2 million cutaneous and 0.2 to 0.4 million visceral leishmaniasis cases per year around the world [2]. More than 90% of visceral leishmaniasis cases are reported in developing countries such as India, Bangladesh, Brazil, Sudan, etc. [2]. Furthermore, this parasitic disease has emerged as a serious infection in human immunodeficiency virus-infected individuals in its visceral

form, accounting for nearly 50% of total visceral leishmaniasis cases reported in Brazil between 2011 and 2013 [3].

For many years, the treatments for leishmaniasis were performed through the use of pentavalent antimonial compounds. However, these compounds are often associated with serious side effects in the kidneys, heart, liver, and pancreas [4, 5]. An effective alternative is the use of amphotericin B (AMPH) and its derivatives for the treatment of various leishmaniasis forms, although they present a high level of toxicity, high cost, and low solubility and bioavailability [5, 6].



► **Fig. 1** Chemical structures of (A) piperlongumine (PPL) and its putative metabolites, (B) Ma, and (C) Mb produced by biomimetic model.

This set of limitations governing current chemotherapies for the treatment of leishmaniasis demonstrates the demand for the discovery of cost-effective drugs. For that, natural products and analogues have offered a remarkable source of compounds in screening for potential antileishmanial drugs [7, 8]. Alkaloids derived from Lauraceae, Solanaceae, Piperaceae, and other angiosperm families are used in folk medicine for the successful management of other neglected diseases and infections [8, 9]. Previous works on *Piper* species revealed that some of their bioactive compounds present antileishmanial activity and may be further explored for the production of new antileishmanial drugs [10]. Piperlongumine (PPL), also called pipartine, is one of these bioactive compounds (► **Fig. 1A**). It is a natural piperidine alkaloid derivative found in *Piper* species, e.g., *Piper longum* L., *Piper tuberculatum* J. (de Jacq.), and *Piper arborescens* Roxb. PPL has shown a broad spectrum of biological activities [11–14], including several tumor cell lines with minimal to no impact in normal cells [14]. In addition, PPL has demonstrated promising activity towards parasite species that cause neglected tropical diseases [15–18]. Its leishmanicidal activity has been reported in promastigote forms of *Leishmania donovani* ( $IC_{50}$  of 7.5  $\mu$ M) [18] and *Leishmania amazonensis* ( $IC_{50}$  of 564.1  $\mu$ M) [15].

Considering this background, the synthesis and evaluation of biological activity of PPL analogues may assist in the development of new leishmanicidal drug candidates [19, 20]. In this sense, biomimetic technologies have assisted in structural diversification of both aromatic and aliphatic compounds through single-step reactions without the presence of protecting groups [21]. Synthetic metalloporphyrins and Jacobsen catalysts aim to mimic *in vivo* metabolism carried out mainly by oxidative enzymes such as cytochrome P450 (CYP450) [21, 22].

In this context, the aim of the present work was to evaluate the leishmanicidal effect of PPL and its derivatives (Ma and Mb compounds; ► **Fig. 1B, C**, respectively) produced by a biomimetic model using metalloporphyrins. We also evaluated the hepatic microsomal stability properties of Ma and Mb for their possible bioavailability.

## Results and Discussion

Biomimetic models have been used in the pursuit of bioactive compounds for drug discovery based on structural diversification and increased product yields [21]. In this sense, Jacobsen and metalloporphyrin reactions were employed in an attempt to reproduce the PPL metabolites formed in human liver microsomes [23]. Among the reaction conditions evaluated, only the reactions

carried out in MeOH and with iodobenzene (PhIO), as the oxidant, led to the production of new compounds (**Table 1S**, Supporting Information).

Jacobsen and the metalloporphyrin-based reactions yielded similar biomimetic products (Ma and Mb). For this reason, we replicated the metalloporphyrin reaction (PPL: [Fe(TCPP)Cl]: PhIO in MeOH) for isolation of Ma and Mb since its active site is similar to CYP450 (**Fig. 1S**, Supporting Information, reaction number 24). These two new compounds were isolated and identified at retention times ( $t_R$ ) of 12.5 and 21.5 min (**Fig. 2S**, Supporting Information), which were named Ma and Mb, respectively.

The identification of the biomimetic reaction products (BRP) Ma and Mb were initiated with HRESI-MS analyses in the positive mode yielding the ions  $m/z$  350.1598  $[M + H]^+$  and  $m/z$  253.1071  $[M + H]^+$  (**Figs. 3S** and **4S**, Supporting Information), respectively. Ma and Mb molecular formulas were determined after obtaining accurate monoisotopic mass information. For Ma, the molecular formula was determined as  $C_{18}H_{23}NO_6$  (error: 1.1 ppm, calculated formula  $C_{18}H_{24}NO_6^+$ , 350.1602), while for Mb, the molecular formula was determined as  $C_{13}H_{16}O_5$  (error: 0.0 ppm, calculated formula  $C_{13}H_{17}O_5^+$ , 253.1071).

Low-energy collision-induced dissociation (CID) MS/MS analyses were performed in order to determine the molecular structure of each compound. The ion  $m/z$  350.1598 of Ma (**Fig. 5S**, Supporting Information) was fragmented to produce second-generation ions. The fragment at  $m/z$  280 resulted from the cleavage of an olefinic bond between C3 and C4. The ion at  $m/z$  252 corresponds to the cleavage between C5 and C6 bond. The fragment at  $m/z$  221 is relative to the amide function cleavage (N-C bond). The ion at  $m/z$  190 was associated with a methoxyl group loss in the cinnamic portion.

NMR experiments ( $^1H$ ,  $^1H$ - $^{13}C$  HSQC and  $^1H$ - $^{13}C$  HMBC) were executed for Ma and Mb (**Tables 1** and **2**; **Figs. 6S–15S**, Supporting Information). The same chemical shifts observed in the PPL spectra were also encountered for Ma, except for methoxylation in the lactam ring carbonyl, a ring cleavage, and a terminal ester (**Figs. 6S–10S**, Supporting Information). With the  $^1H$  experiment, an additional methoxyl group at  $\delta_H$  3.74 ppm was observed (H-16; **Fig. 6S**, Supporting Information). The ester function was confirmed by a long-range correlation observed between a methyl signal at  $\delta_H$  3.74 ppm (*s*-H-3) (► **Table 1**) and a quaternary carbon associated with an ester function's carbonyl at  $\delta_H$  167.4 ppm, via HMBC experiment. Additionally, it is possible to assign alkene signals related to an  $\alpha,\beta$ -unsaturated carbonyl system at  $\delta_H$  5.94 (*dd*,  $-J = 11.4$  and 1.4 Hz) and  $\delta_H$  6.30 ppm (*m*) ppm formatted by amide's cleavage. The remaining  $^1H$ , ( $^1H$ - $^{13}C$ ) HSCQ and ( $^1H$ -

► **Table 1** Chemical shift assignments of PPL ( $^1\text{H}$ ) and the Ma substance ( $^1\text{H}$ , HSQC, and HMBC).

Position	$\delta_{\text{H}}$ (integral; multiplicity; $J$ in Hz)			
	$^1\text{H}$ – PPL	$^1\text{H}$ – Ma	HSQC – Ma	HMBC – Ma
2	–	–	–	–
3	6.03 (1H; <i>dt</i> ; 9.7; 1.8)	5.94 (1H; <i>dd</i> ; 11.4; 1.4)	121.7	28.8
4	7.10 (1H; <i>dt</i> ; 9.7, 4.2)	6.3 (1H; <i>m</i> )	146.8	38.9
5	2.53 (2H; <i>m</i> )	2.89 (2H; <i>dt</i> ; 7.0)	288	38.9/121.7/146.8
6	4.01 (2H; <i>t</i> ; 6.4)	3.56 (2H; <i>dt</i> ; 6.4)	38.9	28.8/121.7/166.1
7	–	–	–	–
8	7.40 (1H; <i>d</i> ; 15.6)	6.26 (1H; <i>d</i> ; 15.6)	120.3	130.3/140.6/166.1
9	7.63 (1H; <i>d</i> ; 15.6)	7.51 (1H; <i>d</i> ; 15.6)	140.6	105.2/120.3/130.3/166.1
10	–	–	–	–
11	6.94 (1H; <i>s</i> )	6.72 (1H; <i>s</i> )	105.2	130.3/140.6/153.4
12	–	–	–	–
13	–	–	–	–
14	–	–	–	–
15	6.94 (1H; <i>s</i> )	6.72 (1H; <i>s</i> )	105.2	130.3/140.6/153.4
16	–	3.74 (3H; <i>s</i> )	51.3	167.4
<i>m</i> -OCH <sub>3</sub>	3.90 (6H; <i>s</i> )	3.89 (6H; <i>s</i> )	56.2	140.6
<i>p</i> -OCH <sub>3</sub>	3.82 (3H; <i>s</i> )	3.87 (3H; <i>s</i> )	61.0	153.4

PPL = piperlongumine, Ma = piperlongumine metabolite produced by the biomimetic model, *s* = singlet, *d* = doublet, *m* = multiplet, *dd* = double doublet, *dt* = double triplet

$^{13}\text{C}$ ) HMBC Ma signals are in agreement with corresponding signals in PPL (► **Table 1**).

The identification of Mb was also performed by  $^1\text{H}$ ,  $^1\text{H}$ - $^{13}\text{C}$  HSQC and  $^1\text{H}$ - $^{13}\text{C}$  HMBC NMR experiments (► **Table 2**; **Figs. 11S–15S**, Supporting Information). It was observed that a methoxylation in the cinnamic carbonyl portion led to the elimination of the lactam ring and formation of a methyl ester. This proposed structure was confirmed by long-range correlation signals between the methoxyl group at  $\delta_{\text{H}}$  3.81 ppm (H-16) and carbonyl's quaternary carbon (H-7) at  $\delta_{\text{H}}$  167.4 ppm and carbon  $\alpha$ -carbonyl (H-8) at  $\delta_{\text{H}}$  117 ppm (► **Table 2**; **Figs. 11S–15S**, Supporting Information). The remaining signals follow the phenolic portion profile as observed with PPL (► **Table 2**).

The PPL *in vitro* hepatic metabolism of humans and rats has been described previously [23, 24]. Two hydroxylated metabolites were identified after incubation with rat liver microsomes [24]. Four metabolites derived from *O*-demethylation, epoxidation, and hydroxylation reactions of PPL with human liver microsomes were described [23]. However, for this work, the oxidation of PPL catalyzed by metalloporphyrin did not mimic the CYP450 reactions.

On the other hand, our previous works with microsomes (CYP450) and biomimetic reactions (Jacobsen and metalloporphyrins) yielded similar results [25, 26]. An example is the hydroxylation at the 5-position of dihydroergotamine observed for both models (CYP450 – human and rat liver microsomes and metalloporphyrin) [25]. However, the major product observed in the biological system, 8'-OH- dihydroergotamine, was not identified in

the biomimetic models. In other cases, biomimetic catalysis produces more metabolites than observed in *in vivo* conditions [26].

Once the structures were determined, Ma, Mb, PPL, and AMPH, a positive control, were evaluated in promastigote forms of *L. amazonensis* and *L. infantum* (► **Fig. 2**). Both *L. amazonensis* and *L. infantum* were susceptible to the compounds, but with differences in their susceptibility rate. Our results also demonstrated a dose-dependent activity in *L. infantum*, with IC<sub>50</sub> values of 7.9, 167.0, 384.2, and 0.58  $\mu\text{M}$  for PPL, Ma, Mb, and AMPH, respectively, after 26 h of treatment (► **Fig. 2**; **Fig. 16S**, Supporting Information). For *L. amazonensis*, similar conditions produced IC<sub>50</sub> values for PPL, Ma, Mb, and AMPH of 3.3, 275.8, 160.5, and 0.86  $\mu\text{M}$ , respectively (► **Fig. 2**; **Fig. 17S**, Supporting Information). Among the tested compounds, PPL was the most effective in both strains. These results are in agreement with the reported IC<sub>50</sub> values for PPL in promastigotes of *L. donovani* [18]. On the other hand, a recent study showed an IC<sub>50</sub> value of 564.1  $\mu\text{M}$  for PPL in promastigotes of *L. amazonensis* [15]. Different incubation conditions may prevent an adequate comparison between these studies.

In the current work, modifications in the PPL structure led to a decrease in antileishmanial activity. A previous study demonstrated that the electrophilicity of the C3–C4 olefin is important for PPL activity [27]. Furthermore, the lack of olefin at C8–C9 is related to the reduction of PPL activity [27]. It was previously observed that the opening of the lactam ring of PPL or the introduction of an oxygen atom caused a significant reduction in leishmanicidal activity [15]. These results demonstrate that the presence of the C3–C4 olefin is critical for PPL activity in *Leishmania* strains.

► **Table 2** Chemical shift assignments of PPL ( $^1\text{H}$ ) and the Mb compound ( $^1\text{H}$ , HSQC, and HMBC).

Position	$\delta_{\text{H}}$ (integral; multiplicity; $J$ in Hz)			
	$^1\text{H}$ – PPL	$^1\text{H}$ – Mb	HSQC – Mb	HMBC – Mb
2	–	–	–	–
3	6.03 (1H; $dt$ ; 9.7; 1.8)	–	–	–
4	7.10 (1H; $dt$ ; 9.7; 4.2)	–	–	–
5	2.53 (2H; $m$ )	–	–	–
6	4.01 (2H; $t$ ; 6.4)	–	–	–
7	–	–	–	–
8	7.40 (1H; $d$ ; 15.6)	6.35 (1H; $d$ ; 15.8)	117.0	129.8/144.9/167.4
9	7.63 (1H; $d$ ; 15.6)	7.63 (1H; $d$ ; 15.8)	144.9	105.4/117.0/129.8/167.4
10	–	–	–	–
11	6.94 (1H; $s$ )	6.75 (1H; $s$ )	105.4	129.8/140.0/144.9/153.4
12	–	–	–	–
13	–	–	–	–
14	–	–	–	–
15	6.94 (1H; $s$ )	6.75 (1H; $s$ )	105.4	129.8/140.0/144.9/153.4
16	–	3.81 (3H; $s$ )	105.4	117.0/167.4
$m$ -OCH <sub>3</sub>	3.90 (6H; $s$ )	3.89 (6H; $s$ )	56.2	105.4/140.0
$p$ -OCH <sub>3</sub>	3.82 (3H; $s$ )	3.88 (3H; $s$ )	60.9	153.4

PPL = piperlongumine, Mb = piperlongumine metabolite produced by the biomimetic model,  $s$  = singlet,  $d$  = doublet,  $m$  = multiplet,  $dd$  = double doublet,  $dt$  = double triplet

PPL and its putative metabolites are also effective in intracellular amastigote forms of *L. amazonensis* (► Fig. 3). PPL, Ma, and Mb reduced the infection index in a dose-dependent manner with IC<sub>50</sub> values of 0.4, 3.2, and 13.4  $\mu\text{M}$ , respectively (► Table 3). The evaluation of toxicity in mammalian cells is essential to determine the safety of the compounds. In this regard, selectivity indexes were obtained for amastigote forms of *L. amazonensis* (> 10 for all tested compounds), demonstrating a low toxicity to mammalian cells [15, 28, 29].

Although the mechanism of action of PPL has not been elucidated, studies performed in tumor cells demonstrated that the cell death can be mediated by an increase in the level of reactive oxygen species (ROS) [14, 30]. PPL and putative metabolites (Ma and Mb) can induce oxidative stress in leishmania-infected macrophages nevertheless, further investigations should be undertaken in order to address the leishmanicidal effect of these compounds [31, 32].

The convenience of therapy and patient compliance are important goals for a successful new treatment for leishmaniasis. The Drug for Neglected Disease initiative (DNDi) established some targets for new candidates for leishmaniasis treatment. A safe oral drug with greater than 90% efficacy for a 10-day treatment is crucial in the case of visceral leishmaniasis [33]. In this context, our previous study predicted favorable pharmacokinetic characteristics of PPL, exhibiting negligible hepatic first-pass metabolism and slow hepatic metabolism catalyzed mainly by CYP3A4 and CYP1A2 isoenzymes with production of four metabolites [23]. Metabolic stability is a key feature for selection of new therapeutic

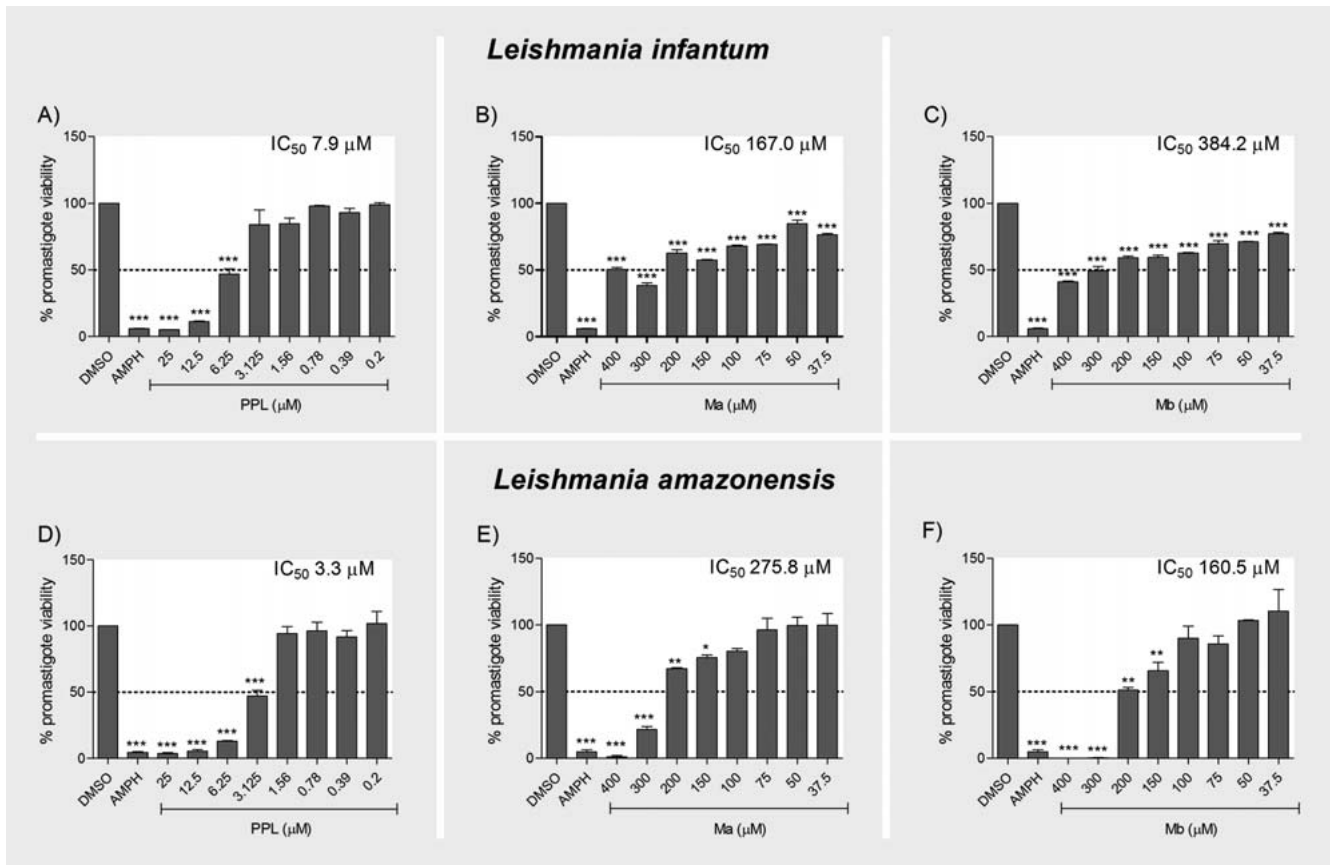
agents. In this sense, the *in vitro* metabolic stability of Ma and Mb was determined in order to predict the *in vivo* metabolic clearance. Examination of the metabolic stability of Ma and Mb employing rat liver microsomes (► Table 4) showed that Ma [half-life ( $t_{1/2}$ ) 180 min] may have a more appropriate plasma exposure than Mb ( $t_{1/2}$  30 min) *in vivo*.

PPL and its derivatives, Ma and Mb, obtained via the metalloporphyrin biomimetic model exhibited leishmanicidal effects in *Leishmania* promastigote and amastigote forms. Among all the compounds examined, PPL showed the highest antileishmanial activity in *in vitro* assays. These results, together with previous pharmacokinetic studies [23], demonstrate the potential of PPL as a candidate for the chemotherapeutic treatment of leishmaniasis. In addition, these results support the development of novel bioactive PPL derivatives in *Leishmania* disease.

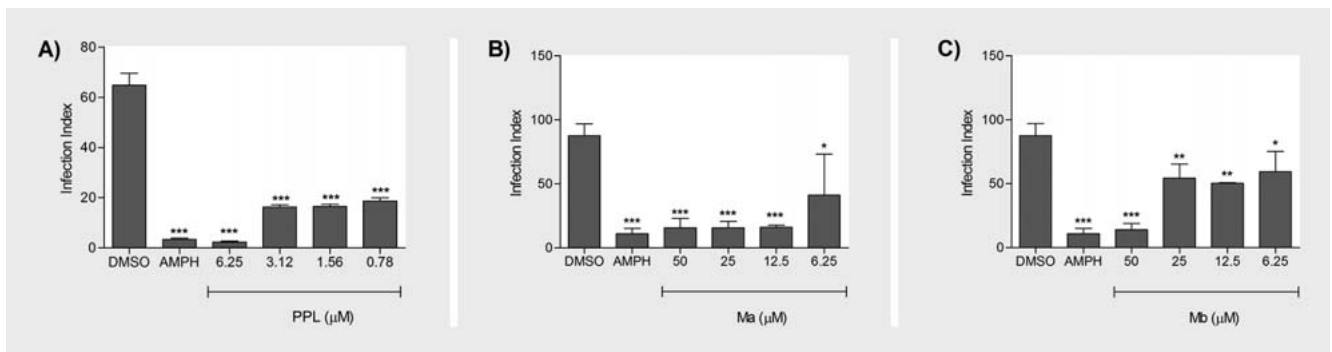
## Material and Methods

### Reagents and solvents

PPL was isolated from *P. tuberculatum* Jacq (Piperaceae) according to a published procedure [16], and the purity studies were performed by Lychnoflora, demonstrating 99% purity. The solvents acetonitrile (ACN), methanol (MeOH), dichloroethane (DCE), and dichloromethane (DCM) of HPLC grade were purchased from Panreac. Deuterated Chloroform (CDCl<sub>3</sub>) was purchased from Sigma-Aldrich. Carbamazepine (purity  $\geq 99\%$ ), used as an internal standard in the metabolic stability assay, was purchased from Sig-



► **Fig. 2** Dose-dependent leishmanicidal activity of PPL (piperlongumine), Ma, and Mb in promastigotes of *L. infantum* (A, B, and C) and *L. amazonensis* (D, E, and F). The results are shown as the percentage of promastigote viability evaluated by the proportional reduction of Alamar blue compared with the drug-free control (DMSO = 0.1%). Amphotericin B (AMPH, 2 μM) was used as the positive control drug. Values represent the mean ± SEM of three replicates from two different experiments; \*p ≤ 0.05, \*\*p ≤ 0.01, \*\*\*p ≤ 0.001.



► **Fig. 3** Effect of (A) PPL (piperlongumine), (B) Ma, and (C) Mb on intracellular amastigotes of *L. amazonensis* evaluated by the infection index (% of infected macrophages × mean number of amastigotes/macrophages). Amphotericin B (AMPH, 2 μM) was used as the positive control drug. Bars represent the mean ± SEM in triplicate from two different experiments; \*p ≤ 0.05, \*\*p ≤ 0.01, \*\*\*p ≤ 0.001.

ma-Aldrich. AMPH (purity ≥ 98%) used in the *Leishmania* assays was provided by Sigma-Aldrich. A Milli-Q Plus System (Millipore) was used to purify water used in the experiments. 3-Chloroperoxybenzoic acid (m-CPBA), (S,S)-, (R,R)-Jacobsen catalyst (Acros Organic), and the organometallic complex [Fe(TCPP)Cl] were a generous contribution from the laboratory of Professor Marilda das

Dores Assis (FFCLRP-USP, Brazil). PhIO was obtained by iodosyl benzene diacetate hydrolysis [34], and the iodometric assay (purity ~ 96%) was employed in assessing its purity [35].

## Oxidation reactions and isolation of biomimetic reaction products

The reactions were performed in an Eppendorf amber flask (2 mL) with mechanical stirring (Vibrax VXR agitator, IKA) at room temperature. The proportion of substrate : catalyst : oxidant used was 6 : 0.3 : 9 mM, respectively. The solvent (0.5 mL of ACN, MeOH, DCE, or DCM), oxidant (PhIO or m-CPBA) and ((*S,S*)- or (*R,R*)-Jacobsen catalyst or [Fe(TCPP)Cl] were evaluated in a total of 24 experiments (Table 1S, Supporting Information). The reactions were stopped after 20 h and analyzed by HPLC (same conditions described in the “Metabolic stability” section). No products were detected in the control reactions carried out in the absence of a catalyst and under the same conditions as catalytic runs.

The reaction selected for isolation of the metabolites in a semi-preparative scale was composed of PPL: [Fe(TCPP)Cl]: PhIO in MeOH (0.5 mL). Fifty identical reactions were performed and the products were isolated using a Shimadzu HPLC system comprised of an SCL-10AVP system controller and SPD-M10A VP (190–800 nm) diode-array detector. The software used in the acquisition of the data was Class VP (Shimadzu). The C18 column was used for separation (250 mm × 20 mm, 10 μm, including a C18 guard column, 10 mm, 5 μm; Phenomenex). An isocratic elution composed of ACN:H<sub>2</sub>O (50:50, v/v) with a flow rate of 9 mL/min was employed and 1 mL of sample was injected. Ma and Mb were collected separately in flasks of 50 mL and dried using a lyophilizer from Liobras.

## Identification of biomimetic reaction products

The isolated BRPs were analyzed in a mass spectrometer HRESI-MS (ultrTOF-Q, Bruker Daltonics) operating in the positive mode. The sample was dissolved in ACN:H<sub>2</sub>O (1:1, v/v) and infused into the ESI source using a syringe pump at 300 μL/min. The acquisition was done using a capillary voltage of 3.0 kV, gas flow of 4 L/min, and desolvation temperature of 180 °C. The drying, nebulizing, and collision gas used was nitrogen. Accurate masses were obtained using TFA-Na<sup>+</sup> 10 mg/mL (sodiated trifluoroacetic acid) as a calibrator agent. For structural elucidation, the isolated compounds were dissolved in CDCl<sub>3</sub> and analyzed in resonance nuclear equipment at 600 MHz (14.1 T magnetic field). <sup>1</sup>H, <sup>1</sup>H-<sup>13</sup>C HSQC, and <sup>1</sup>H-<sup>13</sup>C HMBC experiments and elucidation proposals were based on the PPL standard.

## Animals and parasite cultures

Murine peritoneal macrophages from 8-week-old female BALB/c mice weighing approximately 20 g were obtained from the School of Pharmaceutical Sciences of Ribeirão Preto, University of Sao Paulo. The experimental protocol with BALB/c mice was approved by the Animal Ethics Committee from the University of Sao Paulo, number 15.1.1284.60.2 (approved June 2, 2016). Promastigote forms of *L. amazonensis* (Strain, IFLA/BR/1967/PH8, Fundação Oswaldo Cruz, Belo Horizonte Brasil) and *L. infantum* (Strain, MHOM/BR/74/PP75, Fundação Oswaldo Cruz, Belo Horizonte Brasil) were cultured in Schneider medium (Sigma-Aldrich) supplemented with 20% fetal bovine serum, 1% L-glutamine, 10 UI/mL penicillin, and 10 μg/mL streptomycin at 24 °C.

► **Table 3** Antileishmanial activity, cytotoxicity, and selective index found for the PPL, Ma and Mb in *L. amazonensis*.

Compound <sup>a</sup>	Amastigotes IC <sub>50</sub> (μM) <sup>b</sup>	Macrophages CC <sub>50</sub> (μM) <sup>c</sup>	SI <sup>d</sup>
PPL	0.4	10.0	25
Ma	3.2	188.2	59.4
Mb	13.4	199.0	14.9
AMPH	0.2	N. T.	N. T.

<sup>a</sup>PPL: Piperlongumine; Ma and Mb: piperlongumine metabolites produced by the biomimetic model; AMPH: amphotericin B. <sup>b</sup>Value of inhibitory concentration of 50% of amastigotes of *L. amazonensis*. <sup>c</sup>Value of inhibitory concentration of 50% of the peritoneal macrophage.

<sup>d</sup>Selectivity index (ratio between CC<sub>50</sub> and IC<sub>50</sub>). N. T.: not tested

► **Table 4** Metabolic stability of Ma and Mb in rat liver microsomes.

Compound <sup>a</sup>	Microsomal t <sub>1/2</sub> (min)	Substrate remaining <sup>b</sup> (%)
Ma	180	77
Mb	30	28

<sup>a</sup>Ma and Mb: Piperlongumine metabolites produced by the biomimetic model. <sup>b</sup>The percentage of substrate remaining after 50 min of incubation using time zero as 100%

## Promastigote assay

Log phase promastigotes (2.5 × 10<sup>6</sup> cells/well) were aliquoted in Schneider medium (100 μL/well) into 96-well plates containing each compound diluted in the same medium (100 μL/well). The DMSO concentration in the wells was less than 1%, and the final concentrations in each well of the tested compounds were PPL (0.2–25 μM), Ma and Mb (37.5–400 μM), and AMPH (0.015–2.0 μM). The plates were incubated for 20 h at 24 °C, 5% CO<sub>2</sub>. Alamar Blue (22 μL) was added to each well and the promastigotes were incubated under the same conditions for an additional 6 h. For each experiment, controls, including DMSO (≤ 0.1%) and AMPH (cell death control – 2 μM), were utilized. Fluorescence was measured on a SpectraMax M5 microplate reader (excitation at 550 nm and emission at 630 nm) and normalized after the background fluorescence was subtracted according to the following formula: Fluorescence normalized = (Ft<sub>550</sub> – (Ft<sub>630</sub>\* (Fb<sub>550</sub>/Fb<sub>630</sub>))), where Ft<sub>550</sub> and Ft<sub>630</sub> correspond to the emitted fluorescence signal in 550 and 630 nm for the test compound, respectively; Fb<sub>550</sub> and Fb<sub>630</sub> correspond to the emitted fluorescence signal in 550 and 630 nm for a blank containing medium, respectively.

## Antiamastigote assay

An intraperitoneal injection of 1.5 mL sterile 3% thioglycolate medium was administered in BALB/c mice and peritoneal macrophages were harvested by peritoneal lavage after 96 h using cold RPMI 1640 medium supplemented with 10% fetal bovine serum, 1% L-glutamine, 10 UI/mL penicillin, and 10 μg/mL streptomycin.

The macrophages were washed ( $300 \times g$  for 5 min), counted, and plated at  $1 \times 10^5$ /well in coverslips (Knitell Glass) arranged previously in a 24-well plate in RPMI 1640 medium. Non-adherent cells were washed out with PBS after an incubation of 18 h at  $37^\circ\text{C}$  in 5%  $\text{CO}_2$ . Macrophages were then infected with stationary phase *L. amazonensis* promastigotes at a 5:1 parasite/macrophage ratio and incubated during 24 h with the same conditions in RPMI 1640 medium. Free parasites were removed by washing with PBS, and then treated with 6.25–50  $\mu\text{M}$  of Ma and Mb and 1.56–12.5  $\mu\text{M}$  of PPL, previously diluted in DMSO. The DMSO concentration in wells was less than 0.1%. The plate was incubated under the same conditions for 48 h. For each experiment, controls, including DMSO ( $\leq 0.1\%$ ) and AMPH (cell death control – 2  $\mu\text{M}$ ), were utilized. The cell monolayer was fixed in cold absolute methanol, stained with a fast staining kit (Laborclin), mounted on glass slides with Entellan (Merck), and examined under light microscopy. The percentage of infected macrophages was determined by counting at least 100 macrophages in different microscopic fields. An infection index (percentage of infected macrophages  $\times$  mean number of amastigotes/macrophage) was used to express all results.

### Macrophages *in vitro* cytotoxic assay

Mouse macrophages were obtained as described in the previous section and incubated in complete RPMI 1640 media containing 10% fetal bovine serum, 1% L-glutamine, 10 UI/mL penicillin, and 10  $\mu\text{g}/\text{mL}$  streptomycin in 96-well plates at  $37^\circ\text{C}$  and 5%  $\text{CO}_2$ . The cells were washed with PBS after 24 h, and PPL (1.56–12.5  $\mu\text{M}$ ) and Ma and Mb (6.25–50  $\mu\text{M}$ ) were diluted in RPMI 1640 medium with DMSO, and added to the cell culture for 48 h at 5%  $\text{CO}_2$  and  $37^\circ\text{C}$ . The used DMSO concentration was less than 0.1%. MTT solution (0.5 mg/mL; 100  $\mu\text{L}/\text{well}$ ) was added to the cells after the treatment periods and incubated for 4 h at  $37^\circ\text{C}$ . The supernatant was discarded, and the reaction product was diluted in DMSO. The wells absorbance was read using a SpectraMax microplate reader (Spectramax Plus, Molecular Devices) at 570 nm. All experiments were performed in triplicate on biological duplicates, and the percentage of viable cells was calculated in relation to the untreated control. The 50% cytotoxicity concentration ( $\text{CC}_{50}$ ) was determined by logarithm regression analysis of the data using GraphPad Prism 5.0 software.

### Selectivity index

For calculation of the selectivity index, the ratio of the murine peritoneal macrophages  $\text{CC}_{50}$  to the *L. amazonensis* intracellular amastigotes  $\text{IC}_{50}$  was used.

### Statistical analysis

$\text{IC}_{50}$  values were calculated according to a nonlinear regression using GraphPad Prism 5.0 software from two independent experiments performed in triplicate. The data were analyzed using one-way ANOVA employing GraphPad Prism 5.0. P values of less than 0.05 were used as a cutoff for calculating significance.

### Metabolic stability

Hepatic metabolism of Ma and Mb was evaluated using pooled rat liver microsomes prepared as described previously [24]. The microsomal  $t_{1/2}$  values were measured by monitoring substrate dis-

appearance over time. Briefly, substrate stock solutions were prepared in DMSO and were used at 1% (v/v) final working concentrations. Incubation mixtures (200  $\mu\text{L}$ ) were comprised of substrate ( $\sim 5 \mu\text{M}$ ), rat liver microsomes (1 mg/mL), and phosphate buffer (100 mM, pH 7.4). After 5 min pre-equilibration at  $37^\circ\text{C}$ , reactions were initiated by adding the NADPH cofactor (0.25 mM NADP<sup>+</sup>, 5 mM glucose-6-phosphate, and 0.5 U/mL glucose-6-phosphate dehydrogenase). The reaction mixtures were removed at 0, 5, 10, 20, 30, and 50 min and individually mixed with 200  $\mu\text{L}$  of ice-cold acetonitrile containing the internal standard carbamazepine 210  $\mu\text{M}$  (final concentration). The mixtures were vortexed for 20 s and centrifuged for 5 min at  $2860 \times g$ . The supernatant was removed, and aliquots were injected into the chromatographic system.

A Shimadzu HPLC system composed of an LC-20AT solvent pump unit, a CTO-20A column oven, a DGU-20A5 online degasser, a CBM-20A system controller, and an SPD-30A (190–800 nm) diode-array detector was used to detect the metabolites (Ma and Mb). Injections were accomplished automatically using a 50- $\mu\text{L}$  loop SIL-10AF. The data were collected using the LC solution software SPD-30A PDA utility (Shimadzu). The resolution of Ma and Mb was accomplished at  $32^\circ\text{C}$  on a Shimpack VP-ODS column acquired from Shimadzu ( $250 \times 4.6 \text{ mm}$ , 4.6  $\mu\text{m}$ , particle size). ACN:H<sub>2</sub>O (40:60, v/v) at a flow rate of 1 mL/min was used as the mobile phase under the isocratic mode and 20  $\mu\text{L}$  were injected. The cofactor solution was absent in the control incubations and considered 100% of the activity. The *in vitro*  $t_{1/2}$  was obtained by analyzing the plot of Ln% of remaining activity versus time of incubation. The slope represents the elimination rate ( $k$ ) ( $\text{min}^{-1}$ ) and  $k = -0.693/t_{1/2}$ .

### Supporting information

Biomimetic reaction conditions tested, HPLC chromatograms in analytical and semipreparative scales for the reaction selected, MS and NMR spectra of Ma and Mb, and  $\text{IC}_{50}$ s of AMPH in *L. amazonensis* and *L. infantum* promastigotes are available as Supporting Information.

### Conflict of Interest

The authors declare no conflict of interest.

### References

- [1] Alvar J, Velez ID, Bern C, Herrero M, Desjeux P, Cano J, Jannin J, Boer M. The WHO leishmaniasis control team, 2012. Leishmaniasis worldwide and global estimates of its incidence. PLoS One 2012; 7: e35671
- [2] World Health Organization. WHO to implement online epidemiological surveillance for leishmaniasis, 2016. Available at [http://www.who.int/neglected\\_diseases/news/WHO\\_implement\\_epidemiological\\_surveillance\\_leishmaniasis/en/](http://www.who.int/neglected_diseases/news/WHO_implement_epidemiological_surveillance_leishmaniasis/en/). Accessed August 24, 2016
- [3] Cota GF, Sousa MR, Mendonça ALP, Patrocínio A, Assunção LS, Faria SR, Rabello A. Leishmania-HIV co-infection: clinical presentation and outcomes in an urban area in Brazil. PLoS Neglected Trop Dis 2014; 8: e2816
- [4] Elmahallawy EK, Agil A. Treatment of leishmaniasis: a review and assessment of recent research. Curr Pharm Des 2015; 21: 2259–2275

- [5] de Menezes JPB, Guedes CES, Petersen ALOA, Fraga DBM, Veras PST. Advances in development of new treatment for leishmaniasis. *Biomed Res Intern* 2015; 2015: 815023
- [6] Balasegaram M, Ritmeijer K, Lima MA, Burza S, Genovese GO, Milani B, Gaspani S, Potet J, Chappuis F. Liposomal amphotericin B as a treatment for human leishmaniasis. *Expert Opin Emerging Drugs* 2012; 17: 493–510
- [7] Cheuka PM, Mayoka G, Mutai P, Chibale K. The role of natural products in drug discovery and development against neglected tropical diseases. *Molecules* 2017; 22: e58
- [8] Ndjonka D, Rapado LN, Silber AM, Liebau E, Wrenger C. Natural products as a source for treating neglected parasitic diseases. *Int J Mol Sci* 2013; 14: 3395–3439
- [9] Gutierrez RMP, Gonzalez AMN, Hoyo-Vadillo C. Alkaloids from *Piper*: a review of its phytochemistry and pharmacology. *Mini Rev Med Chem* 2013; 13: 163–193
- [10] Mgebeahuruike EE, Yrjönen T, Vuorela H, Holm Y. Bioactive compounds from medicinal plants: Focus on *Piper* species. *S Afr J Chem Botany* 2017; 112: 54–69
- [11] Zheng J, Son DJ, Gu SM, Woo JR, Ham YW, Lee HP, Kim WJ, Jung JK, Hong JT. Piperlongumine inhibits lung tumor growth via inhibition of nuclear factor kappa B signaling pathway. *Sci Rep* 2016; 6: 26357
- [12] Bharadwaj U, Eckols TK, Kolosov M, Kasembeli MM, Adam A, Torres D, Zhang X, Dobrolecki LE, Wei W, Lewis MT, Dave B, Chang JC, Landis MD, Creighton CJ, Mancini MA, Tweardy DJ. Drug-repositioning screening identified piperlongumine as a direct STAT3 inhibitor with potent activity against breast cancer. *Oncogene* 2015; 34: 1341–1353
- [13] Bezerra DP, Pessoa C, de Moraes MO, Saker-Neto N, Silveira ER, Costa-Loftufo LV. Overview of the therapeutic potential of piplartine (PPL). *Eur J Pharm Sci* 2013; 48: 453–463
- [14] Raj L, Ide T, Gurkar AU, Foley M, Scenone M, Li X, Tolliday NJ, Golub TR, Carr SA, Shamji AF, Stern AM, Mandinova A, Schreiber SL, Lee SW. Selective killing of cancer cells by a small molecule targeting the stress response to ROS. *Nature* 2011; 475: 231–234
- [15] Araújo-Vilges KM, Oliveira SV, Couto SCP, Fokoue HH, Romero GAS, Kato MJ, Romeiro LAS, Leite JRSA, Kuckelhaus SAS. Effect of piplartine and cinnamides on *Leishmania amazonensis*, *Plasmodium falciparum* and on peritoneal cells of Swiss mice. *Pharm Biol* 2017; 55: 1601–1607
- [16] Moraes J, Keiser J, Ingram K, Nascimento C, Yamaguchi LF, Bittencourt CR, Bemquerer MP, Leite JR, Kato MJ, Nakano E. *In vitro* synergistic interaction between amide piplartine and antimicrobial peptide dermaseptin against *Schistosoma mansoni* schistosomula and adult worms. *Curr Med Chem* 2013; 20: 301–309
- [17] Moraes Jd, Nascimento C, Lopes PO, Nakano E, Yamaguchi LF, Kato MJ, Kawano T. *Schistosoma mansoni*: *In vitro* schistosomicidal activity of piplartine. *Exp Parasitol* 2011; 127: 357–364
- [18] Bodiwala HS, Singh G, Singh CS, Dey SS, Sharma KK, Bhutani IP. Anti-leishmanial amides and lignans from *Piper cubeba* and *Piper retroforatum*. *Nat Med* 2007; 61: 418–421
- [19] Wang YH, Wang LT, Hsieh KY, Natschke SL, Tang GH, Long CL, Lee KH. Multidrug resistance-selective antiproliferative activity of *Piper* amide alkaloids and synthetic analogues. *Bioorg Med Chem Lett* 2014; 24: 4818–4821
- [20] Sun LD, Wang F, Dai F, Wang YH, Lin D, Zhou B. Development and mechanism investigation of a new PPL derivative as a potent anti-inflammatory agent. *Biochem Pharmacol* 2015; 95: 156–169
- [21] Cusack KP, Koolman HF, Lange UEW, Peltier HM, Piel I, Vasudevan A. Emerging technologies for metabolite generation and structural diversification. *Bioorg Med Chem Lett* 2015; 23: 5471–5483
- [22] Guengerich FP. Cytochrome P450 and chemical toxicology. *Chem Res Toxicol* 2008; 21: 70–83
- [23] Moreira FL, Habenschus M, Barth T, Marques LMM, Pilon AC, Bolzani VS, Vessecchi R, Lopes NP, Oliveira ARM. Metabolic profile and safety of piperlongumine. *Sci Rep* 2016; 6: 33646
- [24] Marques LMM, da Silva EA jr., Gouvea DR, Vessecchi R, Pupo MT, Lopes NP, Kato MJ, de Oliveira AR. *In vitro* metabolism of the alkaloid piplartine by rat liver microsomes. *J Pharm Biomed Anal* 2014; 95: 113–120
- [25] Bauermeister A, Aguiar FA, Marques LMM, Malta-Júnior JS, Barros F, Callejon DR, Oliveira ARM, Lopes NP. *In vitro* metabolism evaluation of the ergot alkaloid dihydroergotamine: application of microsomal and biomimetic oxidative model. *Planta Med* 2016; 82: 1368–1373
- [26] Niehues M, Barros VP, Emery FS, Dias-Baruffi M, Assis MD, Lopes NP. Biomimetic *in vitro* oxidation of lapachol: a model to predict and analyse the *in vivo* phase I metabolism of bioactive compounds. *Eur J Med Chem* 2012; 54: 804–812
- [27] Adams DJ, Dai M, Pellegrino G, Wagner BK, Stern AM, Shamji AF, Schreiber SL. Synthesis, cellular evaluation, and mechanism of action of PPL analogs. *Proc Natl Acad Sci U S A* 2012; 109: 15115–15120
- [28] Don R, Ioset JR. Screening strategies to identify new chemical diversity for drug development to treat kinetoplastid infections. *Parasitology* 2014; 141: 140–146
- [29] Pink R, Hudson A, Mouries MA, Bendig M. Opportunities and challenges in antiparasitic drug discovery. *Nat Rev Drug Discov* 2005; 4: 727–740
- [30] Liu JM, Pan F, Li L, Liu QR, Chen Y, Xiong XX, Cheng K, Yu SB, Yu ACH, Chen XQ. Piperlongumine selectively kills glioblastoma multiforme cells via reactive oxygen species accumulation dependent JNK and p38 activation. *Biochem Biophys Res Commun* 2013; 436: 87–93
- [31] Fonseca-Silva F, Inacio JDF, Canto-Cavalheiro MM, Menna-Barreto RFS, Almeida-Amaral EE. Oral efficacy of apigenin against cutaneous leishmaniasis: involvement of reactive oxygen species and autophagy as a mechanism of action. *PLoS Negl Trop Dis* 2016; 10: e0004442
- [32] Fonseca-Silva F, Inacio JDF, Canto-Cavalheiro MM, Almeida-Amaral EE. Reactive oxygen species production by quercetin causes the death of *Leishmania amazonensis* intracellular amastigotes. *J Nat Prod* 2013; 76: 1505–1508
- [33] Katsuno K, Burrows JN, Duncan K, Huijsduijnen RH, Kaneko T, Kita K, Mowbray CE, Schmatz D, Warner P, Slingsby BT. Hit and lead criteria in drug discovery for infectious diseases of the developing world. *Nat Rev Drug Discov* 2015; 14: 751–758
- [34] Sharefkin JG, Saltzman H. *Organic Syntheses Collective*. Organic Syntheses, Inc. 1973; 5: 660
- [35] Lucas HJ, Kenedy ER, Forno MW. *Organic Syntheses Collective*. Organic Syntheses, Inc. 1963; 43: 62